CHAPTER 5

QUANTITATIVE METHODS— REFLECTANCE MEASUREMENT

5.1 INTRODUCTION

The percentage of light at *normal* incidence reflected back to an observer (or to an instrumental observation system) from a flat polished surface of a particular ore mineral is the *reflectance*[1] (R or $R\%$) of that mineral. It has already been explained that this parameter is directly related to the optical constants, n and k, through the Fresnel equation (see Section 4.1.2), which is restated here because of its importance:

$$R = \frac{(n - N)^2 + k^2}{(n + N)^2 + k^2} \tag{5.1}$$

where

n = refractive index of the mineral

N = refractive index of the medium into which reflection takes place (when this is air, $N = 1$)

k = absorption coefficient of the mineral

R = reflectance (when $R = 1$ when $R\% = 100\%$)

From the discussion in Chapter 4, it is clear that, for many minerals or other solid materials, reflectance varies as a function of the wavelength of the incident light. Hence, although reflectances have been determined in white light

[1]The term *reflectivity* is used in some articles.

in the past (before the development of more sensitive photosensors), a reflectance value for a substance should be given at a specified wavelength to be meaningful. Furthermore, for all crystalline substances that are not isotropic (i.e., all noncubic minerals), reflectance will commonly vary as a function of crystallographic orientation of the polished surface relative to the vibration direction of the linearly polarized incident light. Thus, although cubic minerals have a single value of reflectance ($R\%$) at a specified wavelength of light, Section 4.2.2 shows that other minerals show maximum and minimum values of reflectance with all possible intermediate values. The origin and significance of the terminology have already been explained, but it is worth recalling. Uniaxial (hexagonal and tetragonal) minerals have two reflectances: R_o, and R_e. Biaxial (orthorhombic, monoclinic, and triclinic) minerals have, in theory, three reflectances, sometimes symbolized R_p, R_m, R_g (where $R_p < R_m < R_g$), but, since only two reflectances are readily measured and one or the other need not be a maximum throughout the visible region, the symbols R_1 and R_2 are preferred. This chapter is concerned with the quantitative measurement of these reflectance values, their physical significance, and their applications in mineral identification.

The "direct" measurement of reflectance requires relatively large specimens and is the kind of method employed in the calibration of standards used in other methods. The intensity of the stabilized light source beam is measured by photometer; then the intensity of this beam is measured when reflected from a relatively large polished surface of the material at angles close to 90°. The plot of R against angle permits such measurements to be extrapolated to obtain the value at 90°. It is not a technique readily modified for use with the microscope, so that reflectance measurements in ore microscopy have centered on comparison with a standard of known reflectance (known from measurement by the direct method).

The methods first developed and marketed by microscope manufacturers for quantitative reflectance measurement under the ore microscope relied on visual comparison of unknown and standard samples. In 1937, Max Berek developed a *slit microphotometer* that employed a field of view divided in two, with the mineral grain on one side and the capability of varying the intensity of illumination on the other. The variable illumination was achieved by an analyzer; that could be rotated to progressively cross or uncross polarizer and analyzer: the angle of rotation of the analyzer was then read when the observer had matched intensity with the sample. Settings were calibrated against standards of known reflectance. The microphotometer developed in 1953 by A. F. Hallimond also relied on visual matching by the observer—this time matching light intensity reflected from a small mirrored surface located in the center of the field of view. The intensity of illumination of this area could be varied until it matched the unknown phase surrounding it in the field of view. Again, the instrument was calibrated using standards of known reflectance. However, as early as 1927, J. Orcel was experimenting with the use of a photoelectric device to measure light reflected from a polished surface under the micro-

scope. This method, in which a photometer reading for a beam of light reflected by the unknown sample is compared with a reading made under the same conditions for a standard sample has proved to be the most suitable for use with the ore microscope. The early measurements were unreliable, however, due to the primitive electronic systems and problems of specimen preparation and standardization. Subsequent developments, particularly the use of the selenium barrier-layer photoelectric cell by Bowie and Taylor (1958) in a series of systematic measurements in "white" light, established that reliable reflectance measurements can be made in this way. Most modern microphotometers are a development of this work started by Orcel but employ photomultipliers for light measurement—devices that are a million times more sensitive than the selenium cell. The discussion of reflectance measurement in the rest of this chapter will, therefore, center on these modern instruments.

The selenium photocell is still used in certain routine work and operates using a photovoltaic effect in which the current generated is directly proportional to the light intensity. The cell is simply arranged in circuit with a galvanometer. The photomultiplier operates from a photoemissive effect such that, when incident photons fall on a cathode, electrons are ejected from it and are attracted to the first of a series of dynodes, positively charged relative to the cathode, at which many more electrons are ejected. This process continues at the other dynodes in the series. The resulting current amplification is again recorded by the deflection of a galvanometer; both analogue and digital readout systems are available. The size of specimen area illuminated and the size of the field sampled by the photomultiplier are limited by a series of stops or diaphragms.

Before we consider the techniques of modern microscope photometry, a number of other general observations should be made, particularly concerning the relationship between the illumination system, the photometer, and the human eye. The phenomenon of spectral dispersion has already been explained (Section 4.2.3) and illustrated in Figure 4.7. Such spectral dispersion curves assume that the intensity of illumination is uniform throughout the visible region and that the response of the eye or artificial monitoring system is independent of the wavelength. Neither of these assumptions is actually true. The intensity of a microscope lamp, or even of light from the sky, is not uniform across the visible region, as illustrated in Figure 5.1. Light from the sky is appreciably more intense toward the blue end of the spectrum. Microscope lamps differ, of course, depending on their construction and operating conditions (factors normally defined by specifying their *color temperature*, see Section 1.2.4). Two examples are given in Figure 5.1, from which it can be seen that microscope lamps show a greater intensity toward the red-yellow end of the visible spectrum. In practice, this means that, to a single observer, ore mineral colors will appear slightly different when observed using different microscopes with different illumination systems. The human eye is also far from being uniformly sensitive as a detector throughout the visible region. It is

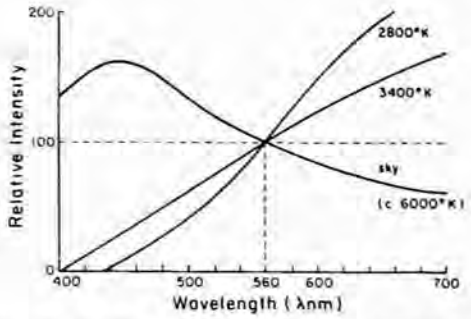

FIGURE 5.1 Spectral curves of the relative intensity (normalized for 560 nm) of the clear sky and for microscope lamps with color temperatures of 2,800 and 3,400°K. (After Galopin and Henry, 1972.)

extremely insensitive at the blue and red ends of the spectrum, with a sensitivity maximum near the center of the visible (~550 nm) portion, as shown in Figure 5.2. When the eye is replaced by a photoelectric device, this too varies in the sensitivity of its response, commonly with a curve similar to that of the eye (Figure 5.2). However, this device in turn is coupled to a galvanometer, which can introduce a further displacement in the zone of maximum sensitivity. In Figure 5.2 are shown the relationships between the absolute intensity of light from a microscope lamp (color temperature 3,400°) reflected from a perfectly "white" surface and the sensitivity of the eye and photometer. Fortunately, of course, in measuring reflectances against standards for which absolute values are known by direct measurement, nonlinearity in source and sensor equally affect sample and standard and therefore cancel. They do, however, affect the sensitivity and accuracy of measurements, which are most reliable in the central region of the visible spectrum.

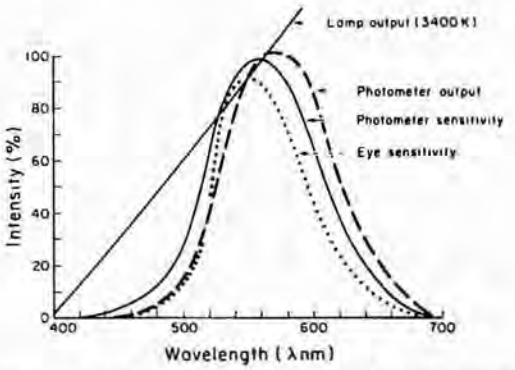

FIGURE 5.2 Sensitivity of the human eye, a typical photometer and a typical photometer measuring system as a function of wavelength. (Modified after Galopin and Henry, 1972.)

5.2 MEASUREMENT TECHNIQUES

As already outlined, reflectance measurements are now performed using photoelectric devices that, for research work, consist chiefly of a photomultiplier tube mounted on the ore microscope. For teaching and certain routine work, the selenium photocell is still employed in simple systems, although robust and inexpensive photomultipliers are now available and give much better results. Whatever photoelectric device is employed, the principal components and their arrangement will be those illustrated in Figure 5.3.

The lamp, which is built into most modern microscope systems, must be run at a high filament temperature (~3,500°K) and should be stabilized for accurate work. In some systems, the *monochromator* is inserted between the light source and the specimen, but in others it is placed immediately in front of the photocell or the photomultiplier. The most convenient and commonly employed monochromator is the interference filter, of which there are two kinds: the *band type* and the *line type*. The band type allows a range of wavelengths with half-height bandwidth of ~20 nm to pass through, whereas, for the line type, the bandwidth is only ~10 nm. Both types are available as single "plate filters" for specified wavelengths or as "running filters" that cover the whole of the visible spectrum. The latter (already calibrated by the manufacturer) is most commonly used on commercial instruments. Even for research work, no greater accuracy is achieved by using a monochromator with a half-height bandwidth less than ~10 nm.

The microscope used in the reflectance-measuring system, commonly a modified modern teaching or research ore microscope, must be fitted with stops or diaphragms to limit the beam (which must be at normal incidence) and the size of area illuminated on the polished section. Most systems are also arranged so that the light from the specimen can pass into the photoelectric device or can be deflected by operating a simple lever and allowing the light to pass through an ocular, enabling the operator to view the specimen.

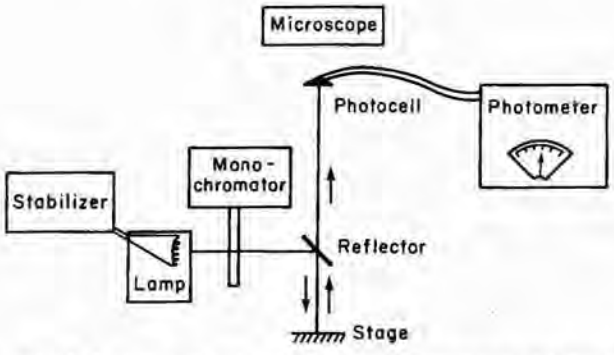

FIGURE 5.3 Block diagram showing the general arrangement for microscope photometry. (After Galopin and Henry, 1972.)

5.2.1 Measurement Procedure

Obviously, precise measurement procedures will vary among different systems, but a typical routine measurement on a simple instrument might involve the following sequence for a reflectance measurement at a specific wavelength in air:

1. Standard and specimen are both carefully cleaned and leveled.
2. An objective is selected (for coarse-grained material a magnification of 8 × to 16 × is most suitable), and the specimen is placed on the stage and sharply focused.
3. A wavelength for measurement is selected (commonly 546 or 589 nm; see Section 5.2.2), and the monochromator is adjusted accordingly.
4. The photometer field stop and the illuminator field stop are adjusted so that the former is about half the diameter of the latter, which in turn covers a homogeneous area of the specimen.
5. The photometer is adjusted so that readings for specimen and standard are both on scale by inserting each in turn and passing the beam through to the photomultiplier photocell.
6. The reading is taken for the specimen by placing it on the stage and passing light to the photomultiplier and taking the galvanometer reading (G'_{sp}).
7. The reading is taken for the standard, which is also carefully focused, with conditions being maintained exactly the same as for the specimen (G'_{st}).
8. If necessary, again with the same conditions maintained, a reading is taken with a black box held over the front of the objective. This is a reading of *primary glare*, which is light reflected from the back surface of the objective before reaching the specimen (C) (see Figure 5.7). Although this correction is recommended in many standard texts, such as Galopin and Henry (1972), in modern instruments such precautions are generally not required (Criddle, 1990).
9. The reflectance is calculated again, if necessary, after the value for the glare measurement has been subtracted:

$$G_{sp} = (G'_{sp} - C) \text{ and } G_{st} = (G'_{st} - C)$$

$$R\%_{specimen} \frac{G_{sp}}{G_{st}} X\, R\%_{standard}$$

The above procedure produces one reflectance value for a specified wavelength, which is all that is required for a cubic (or isotropic noncrystalline) material. If a material is known to be uniaxial, it is possible to prepare oriented polished sections of single crystals cut perpendicular and parallel to the c crystallographic axis so as to measure R_o and R_e and determine the bireflectance

and reflectance sign. Much more commonly, however, the measurements are being made on a randomly oriented aggregate, in which case it is necessary to search for suitable basal and prismatic sections for measurement. Examination under crossed polars to look for a section as near isotropic as possible, and another showing maximum anisotropy, aids the selection. In the latter case, the two extinction positions indicate the two vibration directions; the reflectance is measured for both, one being R_o and the other R'_e (not R_e since we do not know if it is the extreme value). If it is uncertain whether the material is uniaxial, one constant reflectance value in all reliable measurements (i.e., the R_o value present in all general sections) will confirm a uniaxial phase. For a biaxial material of relatively high symmetry (orthorhombic and possibly monoclinic), it is possible to prepare oriented polished sections of coarse single-crystal material. In this way, it is possible to determine R_p, R_m, and R_g (or R_a, R_b, R_c for an orthorhombic crystal). This is specialized work, and more commonly the problem is one of determining reflectances of random grains in a polished section. Any such grain of a material that is at least moderately bireflecting will show two reflectance values that will lie between certain extremes. Unlike the uniaxial material, neither value will be constant from one grain to the next, and it is necessary to search the polished section in order to find values for both R_p and R_g (or R_1 and R_2). In any of these determinations, it is important to make an appreciable number of repeat measurements to ensure consistency of results.

Since most ore minerals exhibit at least some spectral dispersion (Section 4.2.3 and Figure 4.7), reflectance measurement is much more valuable in identification and characterization if readings are taken at several wavelengths through the visible region or if a whole series of measurements are made at regular (say, 20 nm) intervals between 400 and 700 nm so that a spectral reflectance curve can be constructed. In Figure 5.4, stylized spectral reflectance curves are shown to emphasize both the different possible types of curves and the distinction between bireflectance and pleochroism, uniaxial (positive and negative), biaxial, and the use of the symbols R_o, R_e, R'_e, R_1, and R_2. In Figure 5.5, the spectral reflectance curve for pyrite is shown. This is an isotropic phase with a much greater reflectance at the yellow-red end of the visible region, as would be expected from its yellow color. For a uniaxial mineral, it is possible to plot a whole family of curves between the extreme values of R_o and R_e, but in practice only R_o and R_e values are records The example of covellite is shown in Figure 5.6, where spectral curves measured both in air and using an oil immersion objective are shown. In air, the color of the *e* vibration is a pale bluish white—pale because the rise at the end occurs where the sensitivity of the eye is falling rapidly (see Figure 5.2). The *o* vibration is a deep blue, because the proportion of blue light reflected is large compared with yellow light and the steep rise at the end comes where the sensitivity of the eye is declining rapidly. When the covellite specimen is immersed in oil, the shift in R_o to shorter wavelengths is sufficient to introduce an observable red component and the mineral

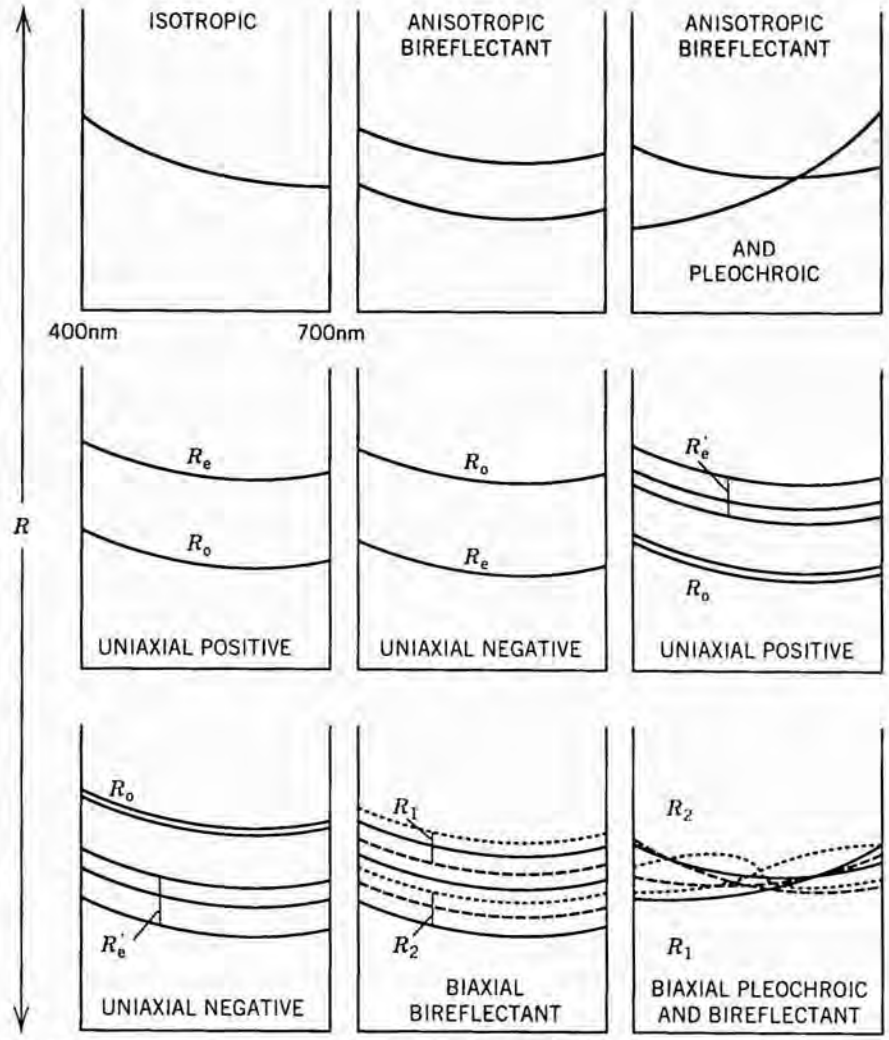

FIGURE 5.4 Stylized reflectance spectra curves illustrating the types of curves and the distinction between bireflectance and reflection pleochroism, uniaxial (positive and negative signs), biaxial, and the use of the terms R_e,R_o,R'_e,R_1,R_2. In all figures, the vertical axis is R and the horizontal axis is wavelength from 400 nm (left) to 700 nm (right). (After Criddle, 1990.)

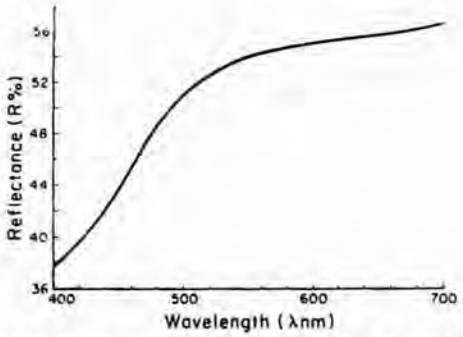

FIGURE 5.5 Spectral reflectance curve for pyrite (FeS_2).

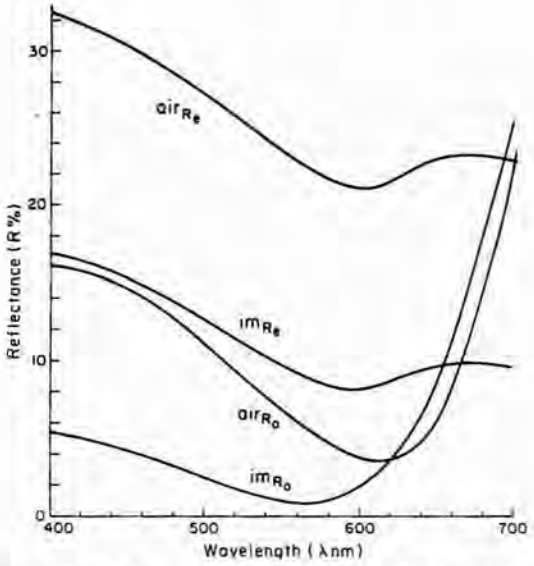

FIGURE 5.6 Spectral reflectance curves for covellite in air and oil immersion (im).

appears a bluish purple.[2] Covellite provides an excellent example of the value of spectral reflectance measurements in understanding the colors of ore minerals in air and in oil immersion. The third example of a spectral reflectance curve shown is that of arsenopyrite, one of the few biaxial minerals for which single crystal-oriented data are available (Figure 5.7). The three vibra-

[2]This phenomenon does not occur in modifications of CuS that differ in details of their crystal structures. These phases were first observed because of their distinctive behavior under oil immersion and initially were called "blue remaining" (or bleiblaubender) covellite. Two minerals have now been characterized by careful work and are named *spionkopite* ($Cu_{1.4}S$) and *yarrowite* ($Cu_{1.12}S$).

tion directions are specified by crystallographic axes, since inspection of the curves will show that assignments of R_g, R_m, and R_p over the entire visible range would be meaningless.

The procedure for making a single measurement that was outlined at the start of this section applies also to the measurement of spectral curves. The modern photomultiplier system is well suited to making measurements throughout the visible spectrum, even on very small grains. In making such measurements, it is possible to measure the standard at all wavelengths initially and then to measure the specimen or to measure each consecutively at each wavelength. The first procedure makes considerable demands on the stability of the apparatus and requires a carefully matched setting of the monochromator at each wavelength. The second procedure is potentially subject to focusing and leveling errors, in addition to problems of returning to the same areas on specimen and standard. However, it is possible to use a specially designed mechanical specimen changer stage, which can be mounted on the microscope. An example of such a device is the *Lanham Specimen-changer Stage* on which specimen and standard can be mounted, leveled, and focused, after which switching between the two is a trivial mechanical operation and both always return to the same area at the same focusing position.

5.2.2 Semiautomated Reflectance Measurement

The measurement procedure just described is such as would be employed on a simple manual instrument However, with the widespread availability of relatively inexpensive, programmable desktop computers, several manufacturers now produce semiautomated instruments. In such systems, after the grain for measurement has been selected and appropriate steps have been taken to ensure adjustment of the microscope itself, measurements can be taken under computer control with a motor-driven monochromator advancing automatically through the selected wavelength range. Multiple scans can be recorded for the sample (and then the standard), stored in the computer, and manipulated to produce reflectance values and spectral dispersion curves (see Criddle, 1990, for further discussion).

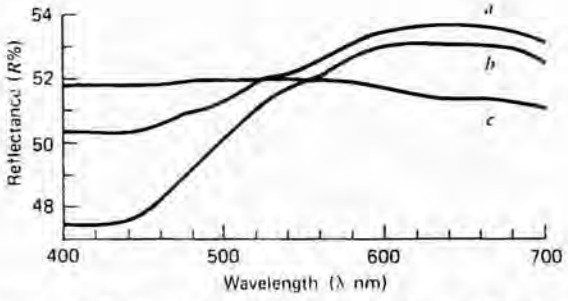

FIGURE 5.7 Spectral reflectance curves of arsenopyrite for vibrations parallel to the main crystallographic directions. (Data from Criddle and Stanley, 1993.)

5.2.3 Standards

Since the widely used methods of reflectance measurement depend on direct comparison of the unknown with a standard of known reflectance, accurate and reliable standards are of the utmost importance. Such matters are the concern of the Commission on Ore Mineralogy (hereafter abbreviated COM) of the International Mineralogical Association, which selected the following materials as standards for reflectance measurement:

Black glass	$R\%$ (air) ~4.5% at 546 nm
Silicon carbide (SiC)	$R\%$ (air) ~ 20% at 546 nm
Tungsten titanium carbide (WTiC)	$R\%$ (air) ~ 50% at 546 nm

These standards, which have been chosen because they can take and maintain a good polish and because they exhibit little spectral dispersion, are obtainable from manufacturers of equipment for microscope photometry, each standard being individually calibrated in air and immersion oil (Cargille D/A oil has been accepted by the COM for measurements made in oil). It is also desirable to employ a standard close in reflectance to the unknown being measured. The standards are relatively expensive, and for routine work it is quite adequate to use a secondary standard, itself calibrated against one of these. The COM has also considered the question of a small number of standard wavelengths for reporting of discrete reflectance values. Such measurements must be made at 470, 546, 589, and 650 nm. If only a single measurement is made, this should be at 546 nm. (This wavelength has been chosen because reflectance values at 546 nm are remarkably close to the luminance value, Y%, for most ore minerals; see Section 5.5).

5.2.4 Errors in Measurement and Their Correction

When you are making a reflectance measurement, it is important to be aware of the errors that can arise and how they can be avoided. These aspects are discussed in much greater detail by Galopin and Henry (1972). Clearly, the light source and photometer must be stable and the photometer reading must be linear before any measurements can be attempted. The specimen should be as well polished as possible, and both specimen and standard must be clean. The reliable calibration of the reflectance standards and of the monochromator are beyond the control of the operator, but the following errors are the responsibility of the user of the instrument.

1. *Leveling errors.* It is very important that both specimen and standard be normal to the axis of the microscope and, for detailed work, that a special specimen stage with leveling screws (e.g., the Lanham stage) be employed. It is possible to check whether the specimen is level by using the *conoscopic leveling test*, in which conoscopic (or convergent) illumination (preferably using the Bertrand lens; see Section 4.3.3.) is employed.

When the illuminator aperture diaphragm is closed down, an image of a spot of light will form in the back focal plane of the objective. The objective used should be of low magnification (< 5×) to obtain a low numerical aperture. When the stage is turned, this image will remain stationary only when the specimen surface is perfectly level.

2. *Focusing errors.* Accurate focusing is also extremely important for good results, and the position of focus must be the same for specimen and standard. The change of height of the reflecting surface over which no loss of image sharpness occurs is called the *depth of focus*, and, within this range, photometer readings do not change. Outside this, a small change in the specimen position produces a large change in the reading. The problem is greatest, therefore, with an objective of large numerical aperture that will have a small depth of focus.
3. *Errors due to setting of the microscope.* The various settings of stops and diaphragms with different objectives can be critical, particularly regarding the problems of *glare* (see Figure 5.8). In the measurement procedure (Section 5.2.1), it was shown how a black box measurement could be used to correct for the effect of primary glare. *Secondary glare* arises from light on its way from the specimen being reflected partly back down by the objective. This light forms a secondary component but one that varies according to the reflectance of the specimen and hence can differ between specimen and standard. This effect can be reduced by using good-quality objectives, by keeping the illuminator field stop fairly small and the photometer field stop only about half this size, and by using objectives of low numerical aperture wherever possible.

5.2.5 Reflectance Measurements in Oil Immersion and the Determination of the Optical Constants *n* and *k*

As already indicated in Section 5.2.1, reflectance measurements can be made in oil. This gives another series of values that may be an aid to identification, but commonly such measurements are undertaken to enable the optical constants, n and k, to be derived by simultaneous substitution in the Fresnel equation (Equation 5.1). Detailed procedures for reflectance measurement in oil

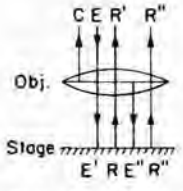

FIGURE 5.8 Primary and secondary glare. Primary glare (C) causes loss of intensity of the incident beam (E), becoming E', which is reflected as R. Secondary glare (E'') produces additional reflection (R''). (After Galopin and Henry, 1972.)

and for solution of the equations to derive optical constants are given in Galopin and Henry (1972), although this method for the determination of n and k suffers from serious error problems (Embrey and Criddle, 1978).

5.3 APPLICATIONS TO MINERAL IDENTIFICATION

The first objective of reflectance measurement is the identification of an opaque mineral. In this regard, a reflectance measurement is the single most useful quantitative optical parameter and is rapidly obtainable using equipment that is easily operated and can be relatively inexpensive to set up. Standards for reflectance determinations are now readily available, so the only other requirements are comprehensive data for ore mineral reflectances and search procedures for utilizing these data. Compilations of reflectance data, often combined with data on Vickers hardness numbers (see Chapter 6), have been published by Bowie and Taylor (1958), Gray and Millman (1962), McLeod and Chamberlain (1968), Galopin and Henry (1972), and Uytenbogaart and Burke (1971). However, as compilations of reflectance data, all of these sources have now been superseded by the data file published by the COM (Criddle and Stanley, 1993). An example of the data presented in this compilation is reproduced in Figure 5.9, from which it can be seen that, as well as the basic information on mineral name, formula, and crystal symmetry, the reflectance ranges in air and oil are given at the four standard wavelengths and detailed spectral curve readings are given at 20 nm intervals from 400 to 700 nm. When available, data are also given on Vickers hardness number and quantitative color measurements (see Section 5.5). Ancillary information on the standard used, the polishing method employed, and the chemical composition of the material may be provided, as well as a reference to the available X-ray data. The data for any single mineral are presented on the top half of the page in the data file; the bottom half has the spectral reflectance curves presented as a plot (see Figure 5.6). Reflectance data at 546 and 589 nm (air) taken from the COM file are provided in Appendix 1 for all of the common ore minerals. A list of these minerals arranged in order of increasing reflectance is also provided in Appendix 2.

The first systems designed to utilize reflectance data in a scheme for ore mineral identification were plots of reflectance against Vickers hardness number. Bowie and Taylor (1958) plotted average reflectance in white light against average microindentation hardness so that each mineral was represented by a point on the chart. Gray and Millman (1962) plotted reflectance in white light against hardness, representing reflectance variations due to bireflectance or compositional variation, so that each mineral appeared as a line on the chart. McLeod and Chamberlain (1968) produced a chart with all available published data, showing both reflectance and hardness variations by intersecting horizontal and vertical lines. However, the original literature has to be consulted if you want to determine whether the data are for white or

Chemical Formula
FeAsS

Symmetry
Monoclinic (pseudo-orthorhombic)

Provenance
Unknown

Standard
SiC (N.P.L. 3AR68)
Monochromator Δλ =
Schott line interference filter

Photomultiplier

Effective N.A.

Air *Oil*

Chemical composition

As	43.1
Fe	34.3
S	20.5
Ba	0.1
wt%	98.0

Quantitative XRF and optical emission spectrographic analysis. (also detected: trace Si, Al, Mg, Ca)

X-ray Data
Diagram corresponds to PDF No. 14–218

λnm	Air R_a	Air R_b	Air R_c	Oil R_a	Oil R_b	Oil R_c
470	50.8	48.7	51.85	34.9	34.4	37.0
546	52.25	51.85	51.9	37.55	37.25	37.2
589	53.25	52.8	51.7	38.4	38.3	37.05
650	53.6	53.0	51.3	39.05	38.9	37.0
400	50.3	47.45	51.8	33.2	31.95	36.55
420	50.3	47.45	51.8	33.45	32.15	36.7
440	50.3	47.55	51.8	33.9	32.55	36.8
460	50.6	48.15	51.8	34.55	33.4	36.95
480	51.0	49.1	51.9	35.3	34.4	37.0
500	51.4	50.1	51.9	36.0	35.4	37.05
520	51.85	51.0	51.9	36.75	36.3	37.15
540	52.15	51.65	51.9	37.4	37.1	37.2
560	52.5	52.2	51.9	37.9	37.7	37.15
580	53.05	52.65	51.8	38.3	38.15	37.05
600	53.45	52.95	51.65	38.65	38.5	37.05
620	53.6	53.0	51.5	38.95	38.8	37.05
640	53.6	53.0	51.3	39.05	38.85	37.05
660	53.6	52.95	51.3	39.1	38.9	37.0
680	53.45	52.75	51.15	39.1	38.8	37.0
700	53.15	52.4	51.0	38.9	38.6	37.0

Colour values

	Air R_a	Air R_b	Air R_c	Oil R_a	Oil R_b	Oil R_c	*Illuminant*
x	.315	.318	.310	.320	.323	.310	C
y	.321	.325	.317	.327	.330	.317	
Y%	52.5	51.8	51.8	37.6	37.3	37.1	
λ_d	579	576	498	577	576	562	
P_e%	2.4	4.5	0.2	5.5	7.0	0.4	
x	.451	.453	.446	.455	.457	.447	A
y	.409	.411	.408	.411	.412	.408	
Y%	52.8	52.2	51.8	38.0	37.7	37.1	
λ_d	587	584	507	585	585	554	
P_e%	3.6	6.5	0.3	7.9	10.0	0.3	

VHN: 1081 on (001) section *Load (gf)* 100
sf

Polishing Method
Grinding: alumina on glass Finishing: alumina on lead, 'microcloth'

Reference & Further Information
Data of P.R. Simpson (1975) QDF (1st ed.) 1. 0520.1 (QDF2.19)
(Data for the four COM wavelengths are interpolated – ed.)
Cargille oil DIN 58.884

FIGURE 5.9 Example of a card from Criddle and Stanley (1993), showing complete reflectance, Vickers microhardness, and quantitative color data for arsenopyrite. Additional information on X-ray data and chemical composition are provided. (Reproduced with permission.)

and for solution of the equations to derive optical constants are given in Galopin and Henry (1972), although this method for the determination of n and k suffers from serious error problems (Embrey and Criddle, 1978).

5.3 APPLICATIONS TO MINERAL IDENTIFICATION

The first objective of reflectance measurement is the identification of an opaque mineral. In this regard, a reflectance measurement is the single most useful quantitative optical parameter and is rapidly obtainable using equipment that is easily operated and can be relatively inexpensive to set up. Standards for reflectance determinations are now readily available, so the only other requirements are comprehensive data for ore mineral reflectances and search procedures for utilizing these data. Compilations of reflectance data, often combined with data on Vickers hardness numbers (see Chapter 6), have been published by Bowie and Taylor (1958), Gray and Millman (1962), McLeod and Chamberlain (1968), Galopin and Henry (1972), and Uytenbogaart and Burke (1971). However, as compilations of reflectance data, all of these sources have now been superseded by the data file published by the COM (Criddle and Stanley, 1993). An example of the data presented in this compilation is reproduced in Figure 5.9, from which it can be seen that, as well as the basic information on mineral name, formula, and crystal symmetry, the reflectance ranges in air and oil are given at the four standard wavelengths and detailed spectral curve readings are given at 20 nm intervals from 400 to 700 nm. When available, data are also given on Vickers hardness number and quantitative color measurements (see Section 5.5). Ancillary information on the standard used, the polishing method employed, and the chemical composition of the material may be provided, as well as a reference to the available X-ray data. The data for any single mineral are presented on the top half of the page in the data file; the bottom half has the spectral reflectance curves presented as a plot (see Figure 5.6). Reflectance data at 546 and 589 nm (air) taken from the COM file are provided in Appendix 1 for all of the common ore minerals. A list of these minerals arranged in order of increasing reflectance is also provided in Appendix 2.

The first systems designed to utilize reflectance data in a scheme for ore mineral identification were plots of reflectance against Vickers hardness number. Bowie and Taylor (1958) plotted average reflectance in white light against average microindentation hardness so that each mineral was represented by a point on the chart. Gray and Millman (1962) plotted reflectance in white light against hardness, representing reflectance variations due to bireflectance or compositional variation, so that each mineral appeared as a line on the chart. McLeod and Chamberlain (1968) produced a chart with all available published data, showing both reflectance and hardness variations by intersecting horizontal and vertical lines. However, the original literature has to be consulted if you want to determine whether the data are for white or

Chemical Formula
FeAsS

Symmetry
Monoclinic (pseudo-orthorhombic)

Provenance
Unknown

Standard
SiC (N.P.L. 3AR68)
Monochromator Δλ =
Schott line interference filter

Photomultiplier

Effective N.A.

Air *Oil*

Chemical composition

As	43.1
Fe	34.3
S	20.5
Ba	0.1
wt%	98.0

Quantitative XRF and optical emission spectrographic analysis. (also detected: trace Si, Al, Mg, Ca)

X-ray Data
Diagram corresponds to PDF No. 14–218

λnm	Air			Oil		
	R_a	R_b	R_c	R_a	R_b	R_c
470	50.8	48.7	51.85	34.9	34.4	37.0
546	52.25	51.85	51.9	37.55	37.25	37.2
589	53.25	52.8	51.7	38.4	38.3	37.05
650	53.6	53.0	51.3	39.05	38.9	37.0
400	50.3	47.45	51.8	33.2	31.95	36.55
420	50.3	47.45	51.8	33.45	32.15	36.7
440	50.3	47.55	51.8	33.9	32.55	36.8
460	50.6	48.15	51.8	34.55	33.4	36.95
480	51.0	49.1	51.9	35.3	34.4	37.0
500	51.4	50.1	51.9	36.0	35.4	37.05
520	51.85	51.0	51.9	36.75	36.3	37.15
540	52.15	51.65	51.9	37.4	37.1	37.2
560	52.5	52.2	51.9	37.9	37.7	37.15
580	53.05	52.65	51.8	38.3	38.15	37.05
600	53.45	52.95	51.65	38.65	38.5	37.05
620	53.6	53.0	51.5	38.95	38.8	37.05
640	53.6	53.0	51.3	39.05	38.85	37.05
660	53.6	52.95	51.3	39.1	38.9	37.0
680	53.45	52.75	51.15	39.1	38.8	37.0
700	53.15	52.4	51.0	38.9	38.6	37.0

Colour values

	Air			Oil			Illuminant
	R_a	R_b	R_c	R_a	R_b	R_c	
x	.315	.318	.310	.320	.323	.310	C
y	.321	.325	.317	.327	.330	.317	
Y%	52.5	51.8	51.8	37.6	37.3	37.1	
λ_d	579	576	498	577	576	562	
P_e%	2.4	4.5	0.2	5.5	7.0	0.4	
x	.451	.453	.446	.455	.457	.447	A
y	.409	.411	.408	.411	.412	.408	
Y%	52.8	52.2	51.8	38.0	37.7	37.1	
λ_d	587	584	507	585	585	554	
P_e%	3.6	6.5	0.3	7.9	10.0	0.3	

VHN: **1081 on (001) section** *Load (gf)* **100**
sf

Polishing Method
Grinding: alumina on glass Finishing: alumina on lead, 'microcloth'

Reference & Further Information
Data of P.R. Simpson (1975) QDF (1st ed.) 1. 0520.1 (QDF2.19)
(Data for the four COM wavelengths are interpolated – ed.)
Cargille oil DIN 58.884

FIGURE 5.9 Example of a card from Criddle and Stanley (1993), showing complete reflectance, Vickers microhardness, and quantitative color data for arsenopyrite. Additional information on X-ray data and chemical composition are provided. (Reproduced with permission.)

monochromatic light reflectances. In the book by Galopin and Henry (1972), a series of charts for different major ore mineral groups show hardness plotted against reflectance, but again in white light. The most recent determinative chart of this type is that of Tarkian (1974) in which reflectance values at 589 nm (air) are plotted against Vickers hardness number, with ranges of both valves incorporated so that the minerals occupy a "box" on the chart. A chart of this type is provided in Appendix 4 but is based on the COM data file.

A number of other determinative schemes have been introduced, including various semiautomated and computerized search procedures. By far the most significant advance for the student, however, has been the introduction of the *Bowie-Simpson system*, which is available as a student's issue (Bowie and Simpson, 1978) containing 33 common ore minerals. Four charts that show the minerals ordered as to increasing reflectance at 546 nm, and then in the same order for the other standard COM wavelengths of 470, 589, and 650 nm, form the nucleus of the system. The style of presentation is illustrated in Figure 5.10, which shows that the reflectance range for each mineral is represented by a horizontal line. Ticks and markings on this line distinguish isotropic, uniaxial, and biaxial species and whether the range shown is due to bireflectance or compositional variation between individual measured grains (see Figure 5.10). Accompanying tables contain data on Vickers hardness and qualitative properties observable under the microscope. Unless the mineral has very distinctive qualitative properties enabling immediate identification, the procedure involves taking a reflectance measurement at 546 nm that may (in combination with the qualitative properties) conclude the identification or reduce the possibilities to a few minerals. In the latter case, measurements at one or more of the other standard wavelengths should permit identification. Only in some cases is it necessary to use the second quantitative technique of Vickers hardness measurement.

Two other determinative schemes that should be mentioned are the Delft scheme, which utilizes punched "property cards" to systematically limit the possible mineral species (Kühnel, Prins, and Roorda, 1976), and the Nottingham interactive system for opaque mineral identification (NISOMI),

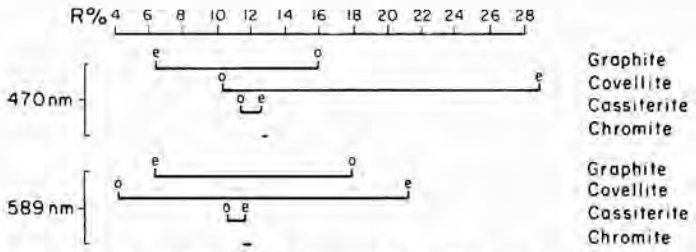

FIGURE 5.10 The Bowie-Simpson system. The reflectance range is represented by a horizontal line, unmarked for an isotropic phase, with ticks (*o* and *e*) for a uniaxial phase and ticks (no letters) for a biaxial phase. (After Bowie and Simpson, 1978.)

which is a series of computer programs that undertake search routines based on input of reflectance and microhardness data (Atkin and Harvey, 1979a). The most recent identification systems, as might be expected, are all built around computerized data bases, and search procedures, and include those described by Gerlitz, Leonard, and Criddle (1989); Hagni and Hagni (1986); and Bernhardt (1987). The subject of identification schemes is critically reviewed by Bernhardt (1990).

5.4 APPLICATIONS TO THE COMPOSITIONAL CHARACTERIZATION OF MINERALS

Reflectance variations and variations in color (which may be treated quantitatively as described in Section 5.5) may be sensitive to variations in mineral composition as well as structural differences. An important and not yet fully explored field is the correlation of reflectance variations with compositional variations in minerals. A number of contrasting examples of this application of reflectance measurements will be considered. The first is the use of a reflectometric method for determining the silver content of natural gold-silver alloys described by Squair (1965) and by Eales (1967). As can be seen from the spectral curves in Figure 5.11, reflectances for pure gold and pure silver show a good separation throughout the visible range with an alloy containing 50% silver having an intermediate reflectance and spectral curve. On the basis of the separation in reflectances of the end members and the range of maximum sensitivity of the microphotometer used, Squair (1965) chose a wavelength of 550 nm at which to measure a series of synthetic alloys and to produce a deter-

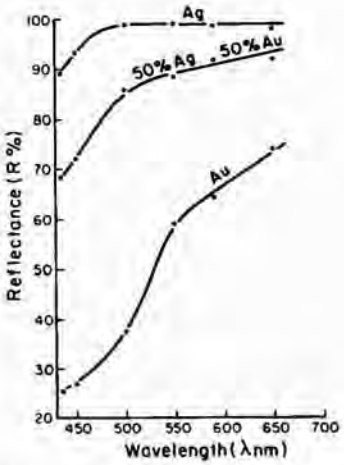

FIGURE 5.11 Spectral reflectance curves of pure gold, silver, and an artificial alloy of 50% gold and silver. (After Squair, 1965.)

minative curve such as that shown in Figure 5.12. Here, the synthetic alloys have been used to plot a curve for the mineralogically important range from 0% to 40% Ag. The reflectances of natural alloys of known chemical composition are also plotted on the figure and give an indication of the accuracy of this method. An important factor in the application of this technique, however, is that the gold should contain no other metal than silver in significant quantities. In particular, copper is known to occur in fairly large amounts in some natural samples and would invalidate the determinative curve. Eales (1967) has also pointed out that gold reflectances are very sensitive to polishing technique.

A number of opaque oxide mineral systems exhibit solid solution behavior, which causes systematic variations in reflectance. An important example is the substitution of magnesium in ilmenite ($FeTiO_3$), which forms a complete solid solution to geikielite ($MgTiO_3$). Cervelle, Lévy, and Caye (1971) have studied the effect of magnesium substitution on reflectance and have developed a rapid method for determination of magnesium content of ilmenite. A series of spectral curves for ilmenites with increasing MgO content are illustrated in Figure 5.13, which shows not only the pronounced effect of this substitution on the reflectances but also that these materials exhibit very little dispersion. This means that a rapid method for magnesium determination can function with a simple white light source. The determinative curve that relates ilmenite reflectance (actually the R_o value present in all sections) to MgO content is shown in Figure 5.14. This rapid method for the determination of magnesium in ilmenites has practical applications in diamond prospecting, since ilmenites from kimberlites characteristically carry ~10% MgO.

In the group of iron sulfide minerals generally termed the "pyrrhotites" and including the stoichiometric end member troilite (FeS) and the metal-defi-

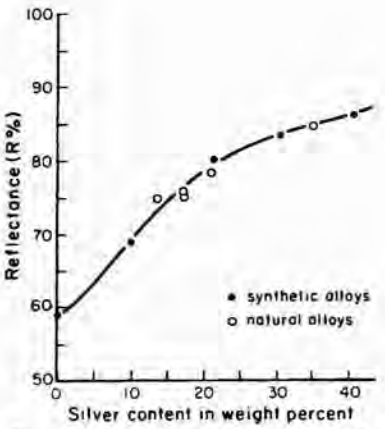

FIGURE 5.12 Plot of reflectance (at $\lambda = 550$ nm) against silver content for synthetic gold-silver alloys. (After Squair, 1965.)

cient "hexagonal" ($\sim Fe_9S_{10}$) and monoclinic ($\sim Fe_7S_8$) pyrrhotites, systematic reflectance variations have been observed as a function of composition. Vaughan (1973) observed a general increase in average reflectance with increasing metal deficiency in a series of synthetic samples. Carpenter and Bailey (1973) demonstrated that measurements of R_o (at 546 nm) could be used to distinguish troilite from "hexagonal" or intermediate pyrrhotite and either of these from monoclinic pyrrhotite.

In the mineralogically very complex series of compositions related to the tennantite-tetrahedrite group, Charlat and Lévy (1976) have examined the reflectivities as a function of complex chemical substitutions in compositions of the type $(Cu,Ag)_{10}(Cu,Fe,Zn,Hg)_2(As,Sb)_4S_{13}$. Although optical properties alone are insufficient to determine chemical composition, they can be used to predict possibilities (e.g., whether the material contains any silver). Typical reflectance curves for the tetrahedrite-tennantite series (after Charlat and Lévy, 1976; Hall, Cervelle, and Lévy, 1974) are shown in Figure 5.15.

Other examples of this systematic approach to the relationship between reflectance and composition include studies of the sulfides and sulfosalts of copper (Lévy, 1967), of the platinum minerals (Stumpfl and Tarkian, 1973), of the silver sulfosalts (Pinet, Cervelle, and Desnoyers, 1978), and of the influence of the Sb content on the reflectance of galena (see Figure 5.16, after Moëlo, 1983).

5.5 QUANTITATIVE COLOR

The colors of ore minerals or other opaque materials observed in reflected linearly polarized light are clearly amongst their major diagnostic features (see Chapter 3). Qualitative descriptions of color are inevitably imprecise and somewhat subjective, so that a system for quantitatively specifying color has

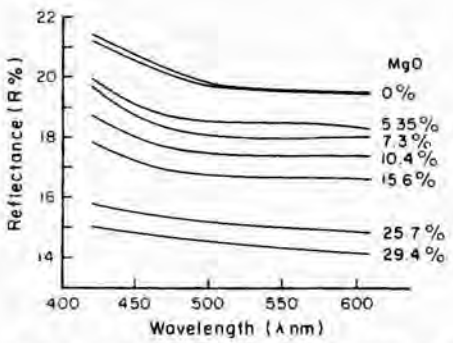

FIGURE 5.13 Plot of reflectance (R_o) for ilmenites with varying MgO contents. (After Cervelle, Lévy, and Caye, 1971.)

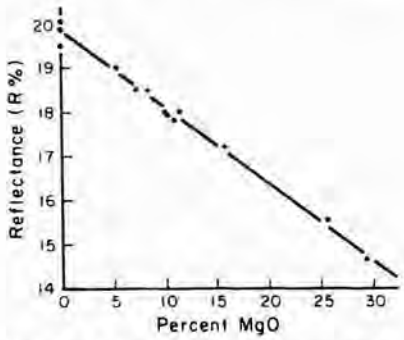

FIGURE 5.14 Plot of reflectance (R %), at about 460 nm, against MgO content for ilmenites ($FeTiO_3$–$MgTiO_3$ series). (After Cervelle, Lévy, and Caye, 1971.)

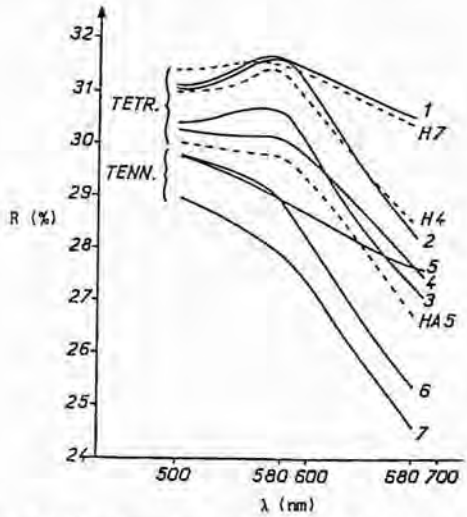

FIGURE 5.15 Typical reflectance curves for tetrahedrite-tennantite series minerals. Compositions are as follows: curves 1 and H7, $Cu_{10}Fe_2Sb_4S_{13}$; curves 2 and H4, $Cu_{10}Zn_2Sb_4S_{13}$; curves 3 and HA5, $Cu_{10}CuFe_2Sb_4S_{13}$; curve 4, $Cu_7Ag_3Zn_2Sb_4S_{13}$; curve 5, $Cu_{10}Fe_2As_4S_{13}$; curve 6, $Cu_{10}CuFeAs_4S_{13}$; curve 7, $Cu_{10}CuFeAs_4S_{13}$. (Data for curves 1–7 from Charlat and Lévy, 1976; curves 4, H7, HA5 from Hall, Cervelle, and Lévy, 1974.)

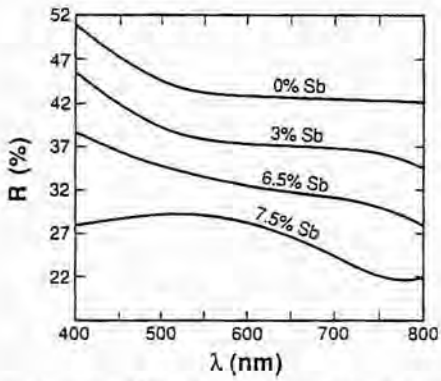

FIGURE 5.16 Reflectance curves for galena with varying concentrations of Sb (after Moëlo, 1983).

obvious advantages. The first publication to deal with color measurements specifically in ore microscopy was that of Piller (1966), although it is only much more recently that the potential of such measurements has been widely appreciated by ore microscopists. In an introductory text, it is not appropriate to go into the details of quantitative color determinations, except to say that the parameters can be easily derived from spectral reflectance data by straightforward calculations. In this section, the theory of quantitative color specifica-

tion is outlined to give a clearer impression of this property and to explain the terminology. Quantitative color data are given, when available, in the COM data file (Criddle and Stanley, 1993) and in Appendix 1 of this book.

The sensation of color, in terms of its subjective perception by the eye, can be described by three attributes—*hue*, *saturation*, and *brightness*. The spectral colors of the visible region (see Figure 4.1) are given names associated with particular wavelength ranges (630–780 nm, red; 450–490 nm, blue, etc.). Each member of this continuous series of colors is a hue; the pure color has maximum (100%) saturation for that hue, whereas white light is regarded in this system of color quantification as having zero saturation. Mixing increasing proportions of white light with a particular hue results in colors of decreasing saturation. The *brightness*, or light intensity of the color, also affects color perception.

It is possible to match any color, as perceived by the eye, by mixing only three spectral colors (e.g., red, green, and blue) in appropriate proportions. The amount of each needed to match a particular color is called the *tristimulus* value for that color. If these values are expressed as fractions summing to unity, they are called *chromaticity* coordinates. The science of color measurement is, of course, well established in other fields, and in 1931 the Commission Internationale de l'Eclairage developed the CIE system based on hypothetical primary colors (X, Y, Z) obtained mathematically from experimental data. The chromaticity coordinates (x,y,z) for any color are positive fractions that sum to unity, so only two need be specified. Commonly, x and y are plotted on orthogonal axes (see Figure 5.17) when the pure spectrum colors fall on an inverted U-shaped curve (the *spectrum locus*), the ends of which are

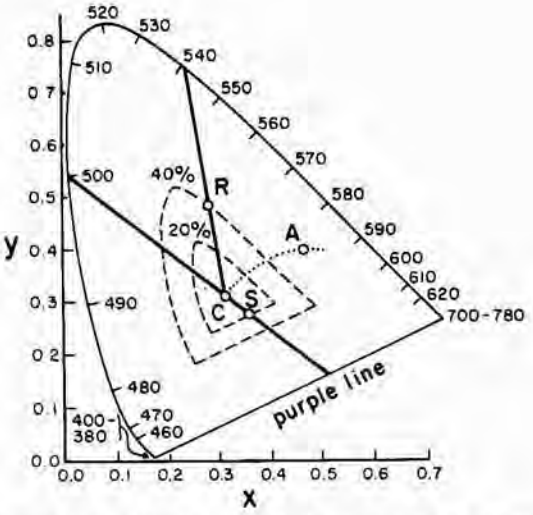

FIGURE 5.17 Chromaticity diagram showing positions of the standard sources (*A*, *C*) and the P_e % λ_d values for two phases (*R*, *S*). (After Htein and Phillips, 1973.)

joined by a straight line (the *purple line*). This line is a locus of colors not found in the spectrum, but the area enclosed by the purple line and spectrum locus encloses chromaticity coordinates for *all* possible colors. The boundary of this area represents the pure colors (100% saturation), whereas a central point within the area represents white (0% saturation). The color sensation produced by an object depends, of course, on the light source used to illuminate it, so the point representing 0% saturation varies with the light source. "Ideal" white light would show the same energy at every wavelength and would plot at coordinates $x = 0.3, y = 0.3$ on the chromaticity diagram (Figure 5.17). However, real light sources differ appreciably from this ideal, so the CIE system specifies several standard white light sources. Source *A* (coordinates $x = 0.4476, y = 0.4075$) corresponds to a tungsten filament microscope lamp, and source *C* corresponds to average daylight ($x = 0.3101, y = 0.3163$) or the microscope lamp, modified by a conversion filter. The color temperatures of these sources are 2,854° K and 6,770° K, respectively, and both are plotted in Figure 5.17.

In determining the chromaticity coordinates for an opaque mineral, it is only necessary to measure the reflectance at a series of wavelengths in the visible range and subject these values to certain mathematical manipulations. However, the chromaticity coordinates are calculated relative to one of the standard illuminants (*A,C*) as a reference achromatic point, and spectral energy distribution values for this source (available from the literature) are needed for the calculation. Although chromaticity coordinates can be calculated for a standard illuminant even when measurements are not made using one of the standard illuminants, conversion of data from one reference illuminant to another requires complete recalculation.

The chromaticity coordinates are a precise means of specifying a color but do not immediately convey any visual impression of the color concerned. From this point of view, two parameters that can be used to specify exactly a point on the chromaticity diagram are more useful. The parameters—*dominant wavelength* (λ_d) and *excitation purity* (P_e)—comprise part of the *monochromatic* or *Helmholtz* system of color specification. These can be illustrated with reference to two examples, *R* and *S*, plotted in terms of their chromaticity coordinates in Figure 5.17. Using the standard *C* illuminant, a line drawn from the point *C* representing this illuminant and passing through the sample point, will intersect the spectrum locus at the dominant wavelength ($\lambda_d = 540$ nm for sample *R*). This is the spectrum color that will match the specimen color when mixed with the "white" of the standard *C* illuminant and therefore conveys an immediate impression of the color concerned. For an example like sample *S*, the corresponding parameter is the *complementary wavelength* (λ_c) and is given by extending the line from *S* to *C* to intersect the spectrum locus (i.e., $\lambda_c = 500$ nm). In this system, the excitation purity is a measure of saturation. It is the distance of the sample point from the achromatic (in this case, *C* illuminant) point expressed as a percentage of the distance to the point on the spectrum locus representing the dominant wavelength (or distance from the

achromatic point to the purple line). P_e % values for samples *R* and *S* are shown as contours on Figure 5.17 and are 40% and 20%, respectively. The one attribute of color not specified by giving chromaticity coordinates or the dominant wavelength and excitation purity is the brightness. A parameter to define this can be incorporated by considering the chromaticity diagram of Figure 5.17 as the base of a three-dimensional figure in which the height above the base (i.e., normal to the *x*-*y* plane) represents increasing brightness on an arbitrary percentage scale. An equivalent parameter is termed the luminance (*Y* %) in the Helmholtz system, where $Y = 100\%$ corresponds to a white light reflectance measurement made with a standard *C* illuminant.

Two other questions that are of particular interest in ore microscopy are: (1) What range of values do the common ore minerals show on a chromaticity diagram? (2) What is the minimum difference in color coordinates that can be detected by the average observer? Both questions can be answered by referring to Figure 5.18, which shows that nearly all of the ore minerals plot in the central portion of the chromaticity diagram. This is a vivid illustration of why many beginning students of ore microscopy see most minerals as gray or white. However, under ideal conditions, the experienced observer can dis-

(*a*)

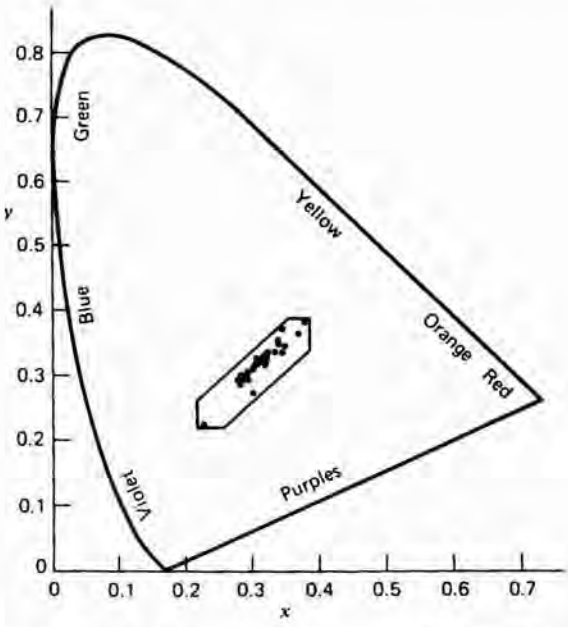

FIGURE 5.18 (*a*) Chromaticity diagram showing the distribution of the chromaticity of all opaque minerals represented in the first issue of the COM quantitative data file for which appropriate data are available. (*b*) Enlargement of the hexagonal area in Figure 5.18a that encloses all chromaticity points of opaque minerals. (After Atkin and Harvey, 1979b; used with permission.) (*c*) Chromaticity diagram showing the discrimination ellipse as it varies in size across the field.

(*b*)

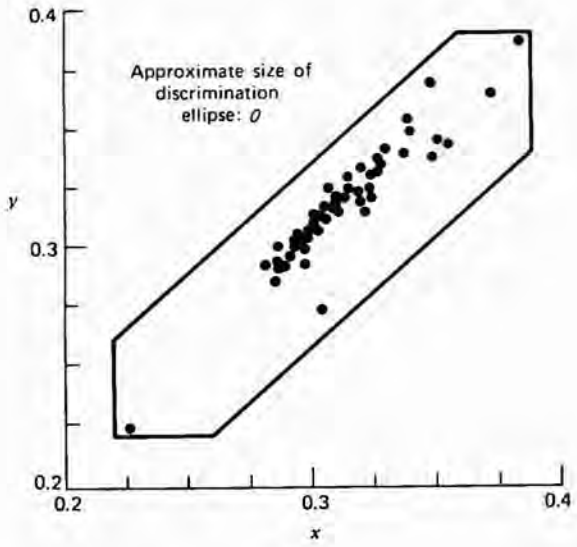

(*c*)

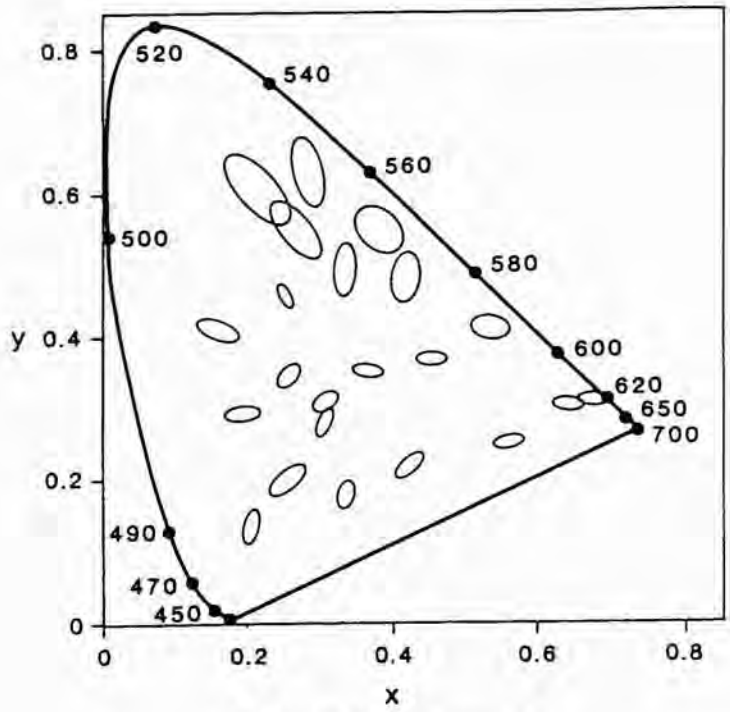

FIGURE 5.18 (*Continued*)

criminate down to the level shown by the *discrimination ellipse*, an example of which is also plotted in Figure 5.18(b). Points plotted inside such an ellipse are indistinguishable from the central color and from each other even under ideal viewing conditions. The discriminatory power of the eye is not, in fact, uniform across the chromaticity diagram, as seen in Figure 5.18(c).

This discussion of quantitative color has necessarily been brief but is enough to illustrate the importance of the topic in ore microscopy. Further information is available in articles by Piller (1966) and Atkin and Harvey (1979a,b), and a book by Peckett (1992). Clearly, the description of the mineral pyrite as $\lambda_d = 573, P_e = 13\%, Y\ \%\ 52.9$ rather than as the color light yellow is an important quantitative advance that will be further stimulated by the availability of reliable quantitative color data in the COM data file.

5.6 THE CORRELATION OF ELECTRONIC STRUCTURE WITH REFLECTANCE VARIATION

Discussions of the theory of light reflection from polished surfaces generally utilize a classical approach based on the Maxwell equations for electromagnetic waves. This approach, essential to the understanding of the refractive index and polarization phenomena, is outlined by Galopin and Henry (1972). However, the classical approach could not explain why, for example, there is a systematic decrease in reflectance (at 496 nm) in the pyrite structure series $FeS_2 \rightarrow CoS_2 \rightarrow NiS_2 \rightarrow CuS_2$. Variations of this type are a result of changes in the *electronic structures* of minerals and materials, and require an explanation related to the description of light as photons rather than as waves (Section 4.1). A simplified approach of this type, based on work by Burns and Vaughan (1970) and Vaughan (1978), can provide a physical picture of the reflecting process, as well as make predictions of reflectance variation with composition possible.

The values of n, k, and hence R (see Equation 5.1) for a solid depend on the interaction of light photons with electrons of the atoms in the solid and therefore on the distribution of electrons in the solid (or its electronic structure). Electrons surrounding an atomic nucleus occur in *orbitals* that are sometimes represented visually as spheres, dumbbell-shaped regions, and so on, centered on the nucleus and within which the probability of the electron occurring is much greater. In simple terms, an electron in an orbital also has a clearly defined energy, and successive electrons added to the system will be at higher energies occupying higher energy orbitals. It is also possible for an electron to be promoted from its normal (*ground state*) orbital energy level to a higher energy empty orbital in a process of *excitation*. This excitation requires energy, which may be a beam of light. When atoms come together to form compounds or minerals, the inner orbitals remain essentially unchanged, but the outermost orbitals overlap to form more complex *molecular orbitals*. Also, the extensive overlap between orbitals in solids causes a broadening of the for-

merly discrete, clearly defined, energy levels into *bands* of closely spaced energy levels. The optical and other electronic properties of materials depend on the nature of the highest energy orbitals or energy bands that contain electrons and the lowest energy empty orbitals. Three important cases can be recognized and are illustrated in the energy level diagrams of Figure 5.19—insulators, semiconductors, and metals.

In an insulator such as pure quartz, the highest orbitals containing electrons (or *valence band* of Figure 5.16) are completely filled with electrons and the only empty orbitals (*conduction band*) into which these electrons could be excited are at much higher energy. It requires a lot more energy than that provided by a beam of visible light to cause such an excitation, and light passes through without being absorbed. In this case, k = zero but $n > 1$ because the light frequency is affected by interaction with the bound (core) electrons. In a metal, the valence band and the conduction band can be envisaged as overlapping (Figure 5.19). Electrons in the highest energy-filled orbitals can readily move to and from the unfilled orbitals, given a small amount of energy (such as visible light energy). A light wave incident on a metal surface may therefore be appreciably absorbed ($k > 0$) as well as slowed down ($n > 1$). In this case, the reflectance is high because light is re-emitted when the excited electrons return to the ground state. This is the case for many metals throughout the visible light range and for many opaque minerals. The semiconductor (Figure 5.19) in its simplest form can be considered an intermediate case between the metal and the insulator. The energy required to excite electrons into the conduction band is greater than in a metal band but much less than in an insulator. Frequently, metal sulfides and oxides are semiconductors that require energies of the order of visible light to produce such excitation.

Electrons excited into the conduction band in a metal or a semiconductor are delocalized and not located on a single atom; that is, they are effectively free and are responsible for the conduction of electricity. The effective number of free electrons (n_{eff}) can be determined; Burns and Vaughan (1970) plotted values of n_{eff} for the pyrite-type FeS_2, CoS_2, NiS_2 and CuS_2 against R% at 496 nm and found a linear relationship. Data available for $CuSe_2$, $CuTe_2$, and Ag also conform with this correlation, which shows that reflectance increases with the effective number of free electrons. In the pyrite-type compounds (see Figure 5.20), the highest energy levels that contain electrons (the 3*d* orbitals of

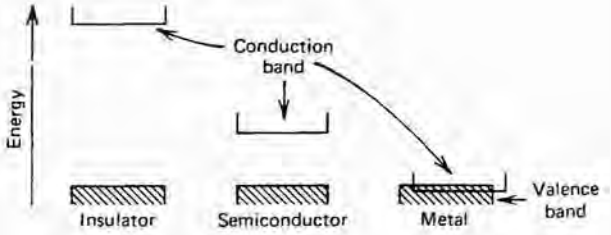

FIGURE 5.19 Energy band structure of insulator, semiconductor, and metal.

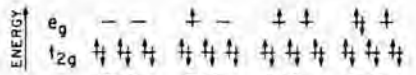

	FeS_2	CoS_2	NiS_2	CuS_2
R% (496 nm)	52	34	27	17
n	2.5	2.5	1.7	2.0
k	3.0	1.8	1.4	0.8
n_{eff}*	2.97	2.08	1.11	0.62

(* for a volume of ~100 Å^3)

FIGURE 5.20 Election occupancy of t_{2g} and e_g energy levels in pyrite-type compounds and the value of reflectance (R%), the optical constants (n and k) and the effective number of free electrons (n_{eff}). (After Burns and Vaughan, 1970.)

the metals) are split into a group of lower-energy and a group of higher-energy orbitals, which are labeled t_{2g} *and* e_g orbitals, respectively. In FeS_2, the t_{2g} orbitals are filled with electrons but the e_g orbitals are empty. The successive addition of electrons across the transition series to CuS_2 results in increased occupancy of the e_g orbitals (see Figure 5.20). These e_g orbitals form a band by overlapping through the crystal (not shown in Figure 5.20), so that electrons excited into the e_g band are delocalized (i.e., become effectively free). As Figure 5.20 shows, both values of n_{eff} and R% systematically decrease in the series $FeS_2 > CoS_2 > NiS_2CuS_2$, and the values of n_{eff} are roughly proportional to the number of empty e_g levels into which t_{2g} electrons may be excited. The reduction in reflectance in the series $FeS_2 > CoS_2 > NiS_2 > CuS_2$ is due to filling of the e_g orbital levels, making fewer of them available for excited electrons that re-emit light energy on returning to the ground state.

The reflectances of these ore minerals are therefore interpreted in terms of their electronic structures and the transition of electrons, which can occur between ground and excited states, resulting in the absorption and re-emission of energy. Certain transitions of this type may or may not occur, depending on the relative orientation of a beam of linearly polarized light and the reflecting crystal. In this way, an interpretation can be offered for the property of bireflectance in substances like graphite and molybdenite. The interpretation of reflectance data for isotropic and anisotropic phases is further discussed by Vaughan (1978, 1990).

5.7 CONCLUDING REMARKS

Reflectance is the single most important quantitative parameter that can be used to identify or characterize an opaque mineral. The availability of efficient and relatively inexpensive instrumentation, good standards, and reliable data for most ore minerals makes reflectance measurement a powerful technique for the ore microscopist. Further development of correlations between compositional variation and reflectance variation should increase the value of the technique, as should the more widespread use of quantitative

color determinations. Interpretation of ore mineral reflectances also offers a challenge to those concerned with understanding the fundamental structures of minerals and a source of further data.

REFERENCES

Atkin, B. P., and Harvey, P. K. (1979a). Nottingham interactive system for opaque mineral identification: NISOMI. *Trans. Inst. Min. Metal.* **88**, 1324–1327.

_____. (1979b). The use of quantitative color values for opaque mineral identification. *Can. Mineral.* **17**, 639–647.

Bernhardt, H.-J. (1987). A simple, fully-automated system for ore mineral identification. *Mineral. Petrol.* **36**, 241–245.

_____. (1990). Microscopic Identification, and Identification Schemes, of Ore Minerals. In J. L. Jambor and D. J. Vaughan (eds.), *Advanced Microscopic Studies of Ore Minerals.* Min. Assoc. Canada Short Course Hdbk, Ottawa, 189–211.

Bowie, S. H. U., and Simpson, P. R. (1978). *The Bowie-Simpson System for the Microscopic Determination of Ore Minerals: First Students Issue.* Applied Mineralogy Group, Mineralogical Society, London.

Bowie, S. H. U., and Taylor, K. (1958). A system of ore mineral identification. *Mining Mag. (Lond.)* **99**, 265.

Burns, R. G., and Vaughan, D. J. (1970). Interpretation of the reflectivity behavior of ore minerals, *Am. Mineral.* **55**, 1576–1586.

Carpenter, R. H., and Bailey, H. C. (1973). Application of R_o and A_r measurements to the study of pyrrhotite and troilite. *Am. Mineral.* **58**, 440–443.

Cervelle, B., Lévy, C., and Caye, R. (1971). Dosage rapide du magnésium dans les ilménites. *Mineral. Deposita* **6**, 34–40.

Charlat, M. and Lévy, C. (1976). Influence des principales substitutions sur les propriétés optiques dans la série tennantite tétraédrite. *Bull. Soc. Franc. Mineral. Crist.* **99**, 29–37.

Criddle, A. J., and Stanley, C. J. (1993). *Quantitative Data File for Ore Minerals*, 3rd ed., Chapman and Hall, London, 635 pp.

Criddle, A. J. (1990). Microscope-Photometry, Reflectance Measurement, and Quantitative Color. In J. L. Jambor and D. J. Vaughan (eds.), *Advanced Microscopic Studies of Ore Minerals.* Min. Assoc. Canada Short Course Hdbk, Ottawa, 135–169.

Eales, H. V. (1967). Reflectivity of gold and gold-silver alloys. *Econ. Geol.* **62**, 412–420.

Embrey, P. G., and Criddle, A. J. (1978). Error problems in the two-media method of deriving the optical constants n and k from measured reflectances. *Am. Mineral.* **63**, 853–862.

Galopin, R., and Henry, N. F. M. (1972). *Microscopic Study of Opaque Minerals.* McCrone Research Associates, London.

Gerlitz, C. N., Leonard, B. F., and Criddle, A. J. (1989). QDF database system. Reflectance of ore minerals—search-and-match identification system for IBM compatible microcomputers using the IMA/COM quantitative data file for ore minerals, second issue. Prog. Abstr. 28th Int. Geol. Congr. Washington D.C. 544-545. U.S. Geol. Surv. Open File Rep. 89-0306A.

Gray, I. M., and Millman, A. P. (1962). Reflection characteristics of ore minerals. *Econ. Geol.* **57**, 325–349.

Hagni, R. D., and Hagni, J. E. (1986). Computer-assisted identification of ore minerals using quantitative and qualitative properties. Program Abstr. 14th Int. Mineral Assoc. Mtg. Stanford, CA, p. 118.

Hall, A. J., Cervelle, B., and Lévy, C. (1974). The effect of substitution of Cu by Zn, Fe and Ag on the optical properties of synthetic tetrahedrite Cu_{12} Sb_4 S_{13}. *Bull. Soc. Franc. Min. Crist.* **97**, 18–26.

Htein, W., and Phillips, R. (1973). Quantitative specification of the colours of opaque minerals. *Mineral. Mater. News Bull. Quant. Microsc. Methods* 1, pp. 2–3; 2, 5–8.

Kühnel, R. A., Prins, J. J., and Roorda, H. J. (1976). The Delft system for mineral identification I. Ore minerals. *Mineral. Mater. News Bull. Quant. Microsc. Methods* 1, 2–3.

Lévy, C. (1967). Contribution á la minéralogie des sulfures de cuivre du type Cu_3. *Mem. Bur. Rech. Géol. Min.* 54.

McLeod, C. R., and Chamberlain, J. A. (1968). Reflectivity and Vickers microhardness. Paper 68-64, *Geol. Surv. Can.*

Moëlo, Y. (1983). Contribution á létude des conditions naturelles de formation des sulfuois complexes d'antimoine et plomb. Document BRGM, Orleans, **55**.

Peckett, A. (1992). *The Colours of Opaque Minerals.* John Wiley & Sons, New York, 471 pp.

Piller, H. (1966). Colour measurements in ore microscopy. *Mineral. Deposita.* **1**, 175–192.

Pinet, M., Cervelle, B., and Desnoyers, C. (1978). Reflectance, indice de réfraction et expression quantitative de la couleur de proustites et pyrargyrites naturelles et artificielles: interpretation génétique. *Bull. Mineral.* **101**, 43–53.

Squair, H. (1965). A reflectometric method for determining the silver content of natural gold alloys. *Trans. Inst. Min. Metall.* **74**, 917–931.

Stumpfl. E. F., and Tarkian, M. (1973). Natural osmium-iridium alloys and iron-bearing platinum: new electron probe and optical data. *Neues Jb. Miner. Monat.*, 313–322.

Tarkian, M. (1974). A key diagram for the optical determination of common ore minerals. *Mineral. Sci. Eng.* **6**, 101.

Uytenbogaardt, W., and Burke, E. A. J. (1971). *Tables for the Microscopic Identification of Ore Minerals.* Elsevier, Amsterdam. (Reprinted 1985 by Dover Publications, New York).

Vaughan, D. J. (1978). The interpretation and prediction of the properties of opaque minerals from crystal chemical models. *Bull. Mineral.* **101**, 484–497.

Vaughan, D. J. (1990). Optical properties and the chemistry of ore minerals. In J. L. Jambor and D. J. Vaughan (eds.), *Advanced Microscopic Studies of Ore Minerals.* Min. Assoc. Canada Short Course Hdbk, **17**, pg. 109–133.